DELFT UNIVERSITY OF TECHNOLOGY

REPORT 13-14

EFFECTIVE WATER STORAGE AS FLOOD PROTECTION
THE RIJNSTRANGEN STUDY CASE

CHRIS BUDD, UNIVERSITY OF BATH
JOEP EVERS, EINDHOVEN UNIVERSITY OF TECHNOLOGY
JASON FRANK, CWI
SARAH GAAF, EINDHOVEN UNIVERSITY OF TECHNOLOGY
RON HOOGWATER, LEIDEN UNIVERSITY
DOMENICO LAHAYE, DELFT UNIVERSITY OF TECHNOLOGY
CORINE MEERMAN, LEIDEN UNIVERSITY
ERIC SIERO, LEIDEN UNIVERSITY
TARA VAN ZALEN, LEIDEN UNIVERSITY

ISSN 1389-6520

Reports of the Department of Applied Mathematical Analysis

Delft 2013

Effective Water Storage as Flood Protection
The Rijnstrangen Study Case

Chris Budd, University of Bath
Joep Evers, Eindhoven University of Technology
Jason Frank, CWI
Sarah Gaaf, Eindhoven University of Technology
Ron Hoogwater, Leiden University
Domenico Lahaye, Delft University of Technology
Corine Meerman, Leiden University
Eric Siero, Leiden University
Tara van Zalen, Leiden University

January 2013

Abstract

Climate change is expected to cause higher discharge levels in the river Rhine at the Dutch-German border. In this study group project that was commissioned by *Rijkswaterstaat*, we investigate the possibility of flooding the Rijnstrangen area as a protective measure. We identify three subproblems. We first analyze the data recorded by *Rijkswaterstaat* and estimate the likelihood and the duration of extremely large discharges at the German border into the river. Next, we investigate how a change in discharge levels affects the water height in the first 35 kilometer section in the Netherlands. Finally we study the design of weirs and floodgates to allow diverting a sufficiently large amount of water flow from the river into the retention area. Our statistical analysis shows that an extreme discharge level is expected to occur once every 1250 years and to last for about three and a half days. Our numerical flow model shows the water height reaches equilibrium on a time scale that is much smaller than the one on which flooding occurs. The flow can thus be considered quasi-stationary. Passive weirs finally are shown to be too long to be feasible. Actively controlled floodgates are therefore recommended.

1 Introduction

The Netherlands is a low-lying country that hosts the estuaries of various rivers, among which the river Rhine. As a large number of people live and work in this delta, the protection of its population and its economic assets are administered at a national level. *Rijkswaterstaat*, part of the Dutch Ministry of Infrastructure and the Environment, is responsible for building and maintaining Dutch infrastructure.

Due to climate change, higher discharge volumes and higher water levels are expected. Certain safety standards specified by Dutch legislation might be violated. *Rijkswaterstaat* therefore has to take action. In this report we focus on the river Rhine. Just downstream from the border with Germany, this river (Upper Rhine or *Bovenrijn*) splits into the *Waal* and the Pannerdens Canal (*Pannerdens Kanaal*), the latter of which again splits into the Lower Rhine (*Nederrijn*) and the *IJssel* (see Figure 1 for a sketch). The ratios of the discharges in the final three branches are regulated by national policy..

The Netherlands has very little influence on the amount of water that enters the country. This is partly due to the uncontrollability of rainfall in upstream parts of the river. Moreover, Germany decides which measures are to be taken (or not) on German territory. The control of flooding of Dutch territory consequently must be achieved in the Netherlands. This SWI group was asked to study one of the possibilities to do so.

Near the cities of Nijmegen and Arnhem and adjacent to the river there is an area called *Rijnstrangen* that potentially serves as a retention area. A retention area is a region surrounded by dikes, intended to serve as a buffer to moderate extremely high discharge volumes. Under normal circumstances, this land is home to people who live and work there with the knowledge that in exceptional cases, they may have to evacuate due to flooding. The Rijnstrangen area could accommodate a maximum capacity of 150 million m^3.

Obviously, turning a region into a retention area has serious consequences. Before this decision can be made, the following issues need to be addressed:

- What is the minimum required capacity of the retention area given the uncertainty in the discharge of the Rhine entering the Netherlands? How does the minimum capacity depend on the peak discharge? *Rijkswaterstaat* would like the discharge peak to be reduced by 500 m^3/s. The retention area should not be completely filled before the extreme discharge event has passed.
- What should the outlets to the retention area look like? Important characteristics are: length, height, location and number. Three types of outlets have been distinguished. The first is a dike that is (partly) demolished in the event of a flood and that needs to be rebuilt afterwards. The second type uses a more sophisticated system of floodgates. For the first two types an authority deciding on the opening of the outlets needs to be installed. The third type is just to have lower dikes locally, acting as a weir. If the water level exceeds the threshold, the retention area will start to fill automatically. In all cases *Rijkswaterstaat* is also interested in having estimates for the water velocities at the outlet;
- What are the consequences of the design of the retention area and the outlets on the discharge ratio in the final three branches of the river?
- How can the retention area be emptied following a flooding event?
- How can people be kept aware of the risks of living and working in the retention area over the course of several centuries? The retention area is only to be flooded under extreme conditions, i.e. very rarely. Most of the inhabitants will eventually perceive the situation to be less serious than it actually is.

These are the issues that the SWI group was asked to consider.

2 Solution approach

The following three subproblems were considered:

1. What is the likelihood and expected duration of an extreme flooding event and what is the total capacity needed to be retained in the Rijnstrangen area? Using statistical analysis of the data provided by *Rijkswaterstaat*, we attempt to estimate these numbers. Methods and results are discussed in Section 3.
2. What are the transient effects, within the Rhine region, of a change in discharge? This question was addressed using a PDE-based shallow water model and numerical simulations. The method and results are presented in Section 4 and Section 5 of this report. The main conclusion is that considering the time scales upon which flooding occurs, the transient effects are negligible.

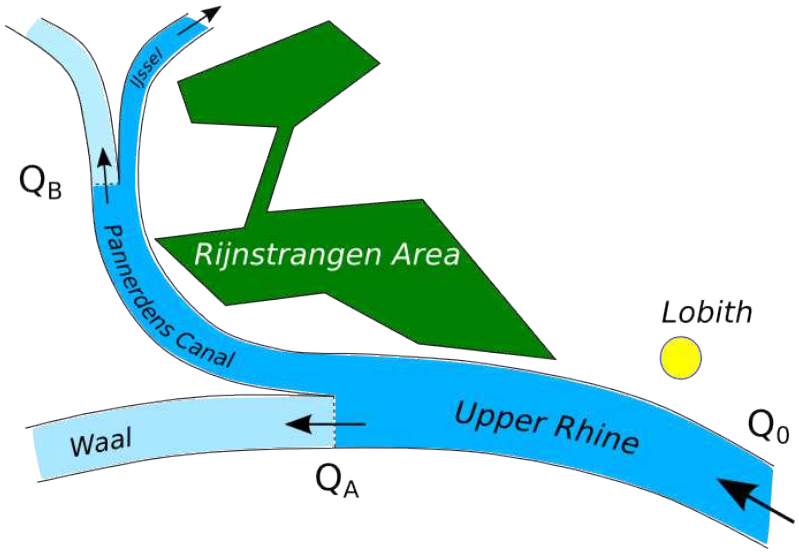

Figure 1: Rhine river system.

3. What options exist for the design of the outlets such that the desired retention capacity is attained? These consist of passive flooding, floodgates and inflow from the bottom of the river. Demolition of a dike was not considered as an outlet option. Models are presented and analysed in Section 6.

3 Basic data analysis

Rijkswaterstaat provided us with a data set of daily discharge measurements at Lobith where the Rhine enters the Nethertlands. We want to derive from this data a model to describe and, more importantly, to predict extreme events. The extreme event in which we are interested is the occurrence of a very high discharge. In this section we will treat two approaches: a more theoretical investigation of extreme events (Section 3.1) and a hands-on interpretation of the data (Section 3.2).

3.1 Distribution of extreme events

In this section we will elaborate the theory of extreme events. We will first introduce a distribution that can be used to describe extreme events. Using this distribution and the available data we will be able to comment on the likelihood of an extreme event to occur.

3.1.1 Generalized extreme value distribution

Discharge Q in m^3/s at Lobith is recorded daily. The available data set of daily measurements of Q contains values from 1 January 1989 to 21 July 2012. To analyse the extreme discharge values we use the 23-year data from 1 July 1989–30 June 2012.

Now we define the vector $\hat{Q}_{\max}$ as the vector of length 23 containing the maximum discharge values at Lobith of each of the given 23 years.

We want to model the yearly maximum discharge at Lobith. This can be done, as described in [2], with the Generalized Extreme Value distribution (GEV distribution), which is defined as

$$G(x) = \exp\left[-\left(1+\gamma\frac{x-\mu}{\sigma}\right)_+^{-\frac{1}{\gamma}}\right], \tag{1}$$

where the notation $F(x)_+$ must be interpreted as

$$F(x)_+ = \begin{cases} F(x) & \text{if } F(x) > 0, \\ 0 & \text{otherwise.} \end{cases} \tag{2}$$

In this work we will assume that $\gamma \downarrow 0$. In the limit the GEV distribution converges to the Gumbel distribution. It is also called the Type I extreme value distribution and it is given by

$$F(x;\mu,\sigma) = e^{-e^{-z}}, \quad \text{where} \quad z = \frac{x-\mu}{\sigma}, \tag{3}$$

as is stated in [2] and the references therein. To this cumulative distribution function (cdf) belongs the probability density function

$$f(x;\mu,\sigma) = \frac{1}{\sigma}e^{-z-e^{-z}}, \quad \text{where again} \quad z = \frac{x-\mu}{\sigma}. \tag{4}$$

Other distributions are for example the Generalized Pareto Distribution (GPD) which is used together with the Peaks Over Threshold (POT). However, we will not work with these distributions for the following reason. In order to work with independent extreme values, [2] proposes that the distance between two peaks above some threshold should be at least 100 days. Assume that we extract from our relatively small amount of data a set of peaks that are at least a distance of 100 days apart. It then follows that these peaks nearly all coincide with the annual maxima. Therefore, due to our small data set, the GPD and the GEV distributions can be used almost interchangeably. In this paper we have chosen to work with the GEV distribution, considering only the yearly maxima, since the extreme values are those we are interested in.

To obtain a reliable estimate of the parameters it is important that the maximum values are independent and a sufficiently large number of extremes is used. We assume in this paper that the maximum values in $\hat{Q}_{\max}$ are independent, since these maximum values are taken over the period of a year. Seasonal trends, for example, will therefore have no influence on the maximum values. It is also important that we defined a year from July to June, since therefore the winter—the season in which extreme values are typically observed—is in its entirety contained in a single year. Notice that our analysis is based on a small set of extreme values as a consequence of a limited amount of available data. We observe here that our estimates are based on a small set of measurements and that they therefore might lack accuracy.

We use this data taking into account that our estimates are based only on a small set and therefore might not be as accurate as desired.

We fitted the Type I extreme value distribution to our measurements. We obtain the following estimates of the mean (the location parameter μ) and standard deviation (the scale parameter σ) from the fitted distribution

$$\sigma = 1\,625.4 \text{ m}^3/\text{s} \quad \text{and} \quad \mu = 5\,965.3 \text{ m}^3/\text{s}. \tag{5}$$

The estimates here are maximum likelihood estimators.

In Figure 2 we plotted the empirical cumulative distribution function for the vector $\hat{Q}_{\max}$ containing the yearly maximum discharge values. The empirical cdf is defined as the proportion of the yearly maximum discharge values Q_i in $\hat{Q}_{\max}$ less than or equal to a certain Q. We plotted also the theoretical cdf (3), using the approximate values μ and σ we obtained. Taking *Rijkswaterstaat*'s

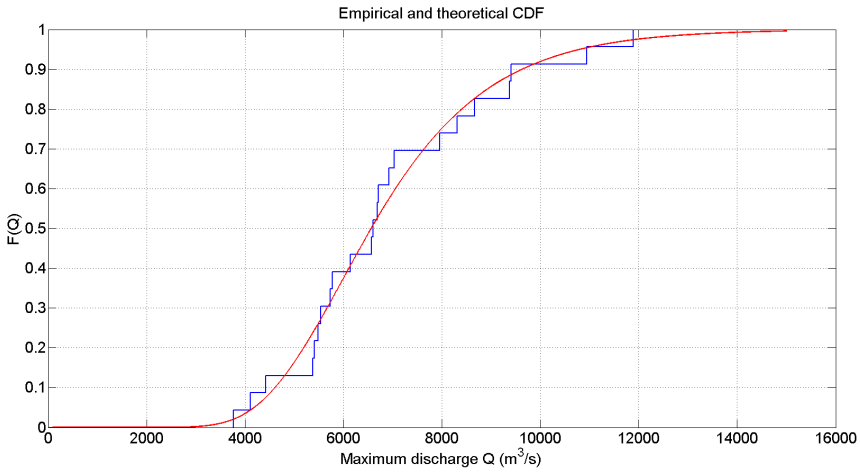

Figure 2: Empirical and theoretical (fitted) cumulative Type I distribution function for the yearly maximum discharge values of 23 years.

proposed threshold value $Q^* = 17500$ m^3/s, we also can calculate the probability that the yearly maximum discharge value exceeds Q^*:

$$\mathbb{P}(Q > 17500) = 8.2763 \cdot 10^{-4}. \tag{6}$$

Yet, this does not really tell us something practically. In the sequel, we will introduce the return period which will give a more explicit expression for the probability of the the occurrence of an extreme event.

As for now it can be seen that the empirical distribution nicely coincides with the theoretical distribution. Taking into account the limited amount of data, the agreement between the empirical cdf and the theoretical distribution is satisfactory.

However, plotting the corresponding probability density function (4) of the Type I extreme value distribution gives a less satisfactory outcome. In Figure 3 and Figure 4 we show the distribution of $\hat{Q}_{\max}$ in the form of a histogram together with the pdf scaled to our data vector $\hat{Q}_{\max}$ of length 23 and to the histogram intervals.

We already stated that the amount of data we use might not yield estimates of the satisfactory accuracy. In fact, the blocks of the histogram corresponding to the empirical data in Figure 3 follow the fitted and scaled pdf and can be considered acceptable, but the histogram in Figure 4 with interval lengths 1000, does not follow the fitted and scaled pdf in a way we would like. In order to obtain more satisfactory results we need more data.

3.1.2 Return level and return period

Other interesting information we can extract from our data relates to the return period. Let $0 < p < 1$. The return period $\frac{1}{p}$ is an estimate of the likelihood of a flood event. The return level z_p associated with the return period is the value that the annual maximum will exceed with probability p. The return level z_p is defined as

$$z_p = \mu - \sigma \log(-\log(1-p)). \tag{7}$$

Remark: this z_p corresponds to the case in which $\gamma = 0$, i.e. to the case of the Type I extreme value distribution. For the exact derivation see [2] and the references therein.

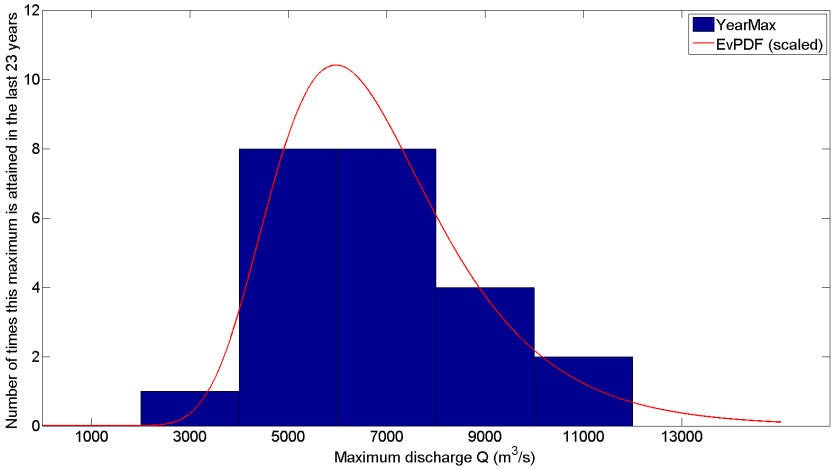

Figure 3: Histogram intervals of length 2000 and the probability density function scaled to our data vector $\hat{Q}_{\max}$ and the histogram intervals.

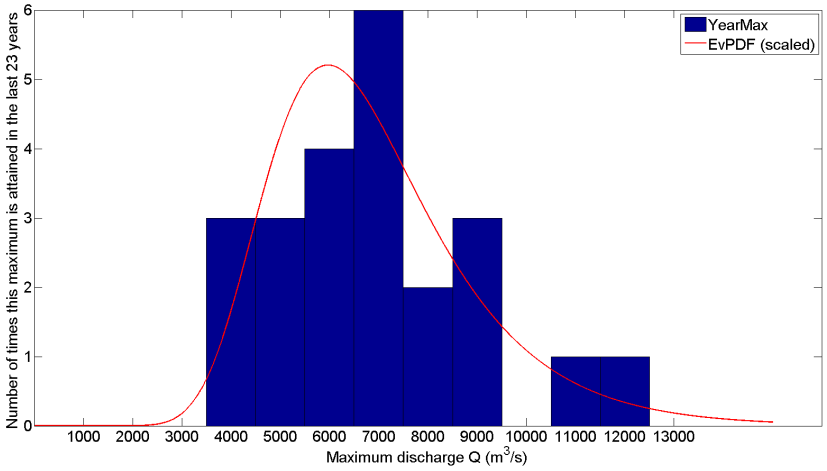

Figure 4: Histogram intervals of length 1000 and the probability density function scaled to our data vector $\hat{Q}_{\max}$ and the histogram intervals.

In Figure 5 the return level is plotted against the return period with a logarithmic scale. According to statistical calculations of *Rijkswaterstaat*, the Dutch dikes have been constructed such that they can deal with exceptional discharges that occur once in 1250 years. The threshold value is recalculated every five years, based on currently available statistical data. In the last decades extreme discharges have become more frequent, and thus the the threshold was increased several times. In 2001 the level was adjusted to 16000 m^3/s (which is the current standard). Due to climate changes, it is expected that this exceptional water level will increase even more. Our model (based on data until 2012) predicts that the return level for the choice of $p = \frac{1}{1250}$ equals $z_p = 17\,555\ \mathrm{m}^3/\mathrm{s}$, as indicated in the figure. This means that with probability $p = \frac{1}{1250}$, i.e. once every 1250 years, this discharge value $z_p = 17\,555\ \mathrm{m}^3/\mathrm{s}$ will be exceeded. Our prediction thus confirms that the threshold value will probably need to be adapted more in the coming years.

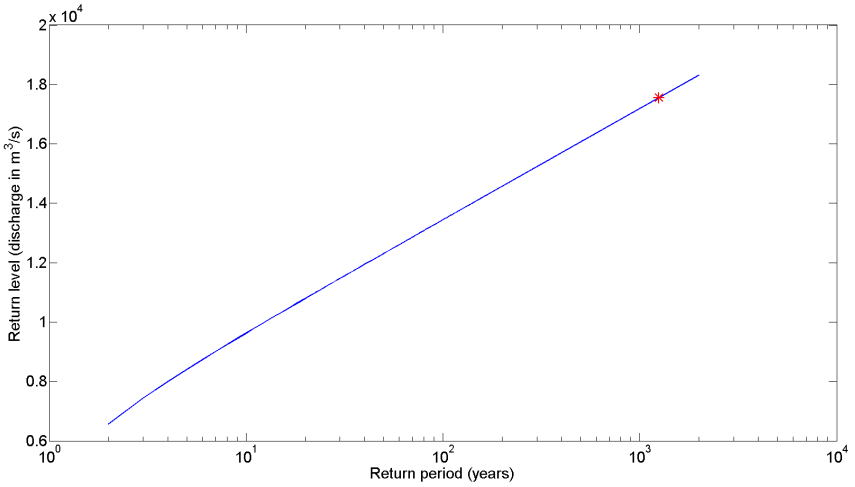

Figure 5: The return level $z_p = 5965.3 - 1625.4 \cdot \log(-\log(1-p))$ associated with the return period $\frac{1}{p}$. With probability $p = \frac{1}{1250}$, i.e. once every 1250 year, the discharge value $z_p = 17\,555$ m^3/s will be exceeded (red star).

Up to now our starting point was the underlying theory for extreme events. In the following section, we explore what information can be deduced from the data in a more *ad hoc* manner.

3.2 *Ad hoc* data analysis

In the previous section we considered extreme events (i.e. high discharge) and their return times. In this section we ask the question: if such an extreme event occurs, what can we say about the amount of time the discharge remains above a certain threshold level Q^*? This information is very useful if at a certain moment we decide to influence the natural discharge. We can do this by allowing water to flow into the retention area Rijnstrangen. Now, consider the situation that we do not want the discharge to exceed some Q^*. This means we need to remove the excess of water effectively. Our aim in this section is to predict how much water the retention area must be able to contain.

3.2.1 Interval length and water volume above threshold

Here, we formulate more precisely what was said in the introduction of this section.

We fix a threshold Q^* and we open the outlets to the retention area if the current discharge Q exceeds Q^*. Let us assume that our actions work effectively enough to make sure that the discharge (in the river) directly downstream of the outlet to the retention area is $\min(Q, Q^*)$.

As said before, we use the daily discharge measurements at Lobith. After Q^* has been fixed, the data set contains a number of intervals in which the measured discharge exceeds Q^*. As in the previous section, we want to consider independent extreme events and to achieve this we only consider those intervals for which the corresponding maximum $Q_{\max}$ is also an annual maximum. The intervals we consider are of *maximal length*. By this we mean that the last measurement before the start of the interval and the first measurement after the interval are smaller than Q^*. In Figure 6 we show an example of such an interval. We determine its boundaries by calculating the intersection of the horizontal line $Q = Q^*$ with the linearly interpolated continuation of measurement data. The interval length L follows from these interval boundaries.

Linear interpolation of the measurements determines a graph (t, Q). The area under this graph but above the line $Q = Q^*$ equals the excess amount of water carried by the river during the period in which $Q > Q^*$. This is exactly the amount of water that needs to be stored in the retention area. We calculate this area by applying the trapezoidal rule to the measured data. In Figure 6 this is the shaded grey area.

Note that this integration procedure has to be executed with some care, since the units of Q (m^3/s) and t (days) do not match.

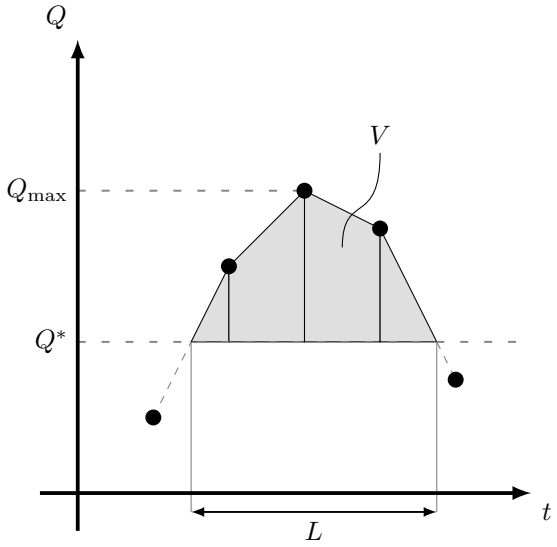

Figure 6: Schematic illustration of how we derive information about the interval length L and total volume V from the measurements. Measured data is indicated by the black circles.

Now, consider those peaks for which the maximum corresponds to an annual maximum. Let us focus on one such peak (with maximum value $Q_{\max}$), and define $\tilde{Q} := Q_{\max} - Q^*$. From the measured data, we calculate $L(\tilde{Q})$ and $V(\tilde{Q})$ by the procedure described above. By varying Q^* one can investigate the relation between $\tilde{Q}$ and L or V, respectively. In Figure 7 we collect this data for all peaks corresponding to annual maxima.

Let $\tau = 86400$ be the number of seconds in a day. One can show that theoretically $L(\tilde{Q})$ and $V(\tilde{Q})$ are related by

$$V(\tilde{Q}) = \int_0^{\tilde{Q}} \tau\, L(\bar{Q}) d\bar{Q}, \tag{8}$$

or, as a result,

$$\frac{dV(\tilde{Q})}{d\tilde{Q}} = \tau\, L(\tilde{Q}). \tag{9}$$

This implies that we can derive from the data relations $(\tilde{Q}, L(\tilde{Q}))$ and $(\tilde{Q}, V(\tilde{Q}))$, but these relations are not mutually independent. A first attempt might be to fit a parabola to the data in Figure 7, right. Then (9) implies that a linear relation should hold in Figure 7, left. The resulting (least squares) fits are indicated in Figure 8.

The linear fit in Figure 8, left, seems justifiable for large $Q_{\max} - Q^*$. However, for $Q_{\max} - Q^*$ near zero the fit is poor. Note that from a practical point of view, we are mostly interested in obtaining information around $Q_{\max} - Q^* \approx 500$. This is because *Rijkswaterstaat* has in mind a situation where $Q_{\max} = 18000$ m^3/s and $Q^* = 17500$ m^3/s.

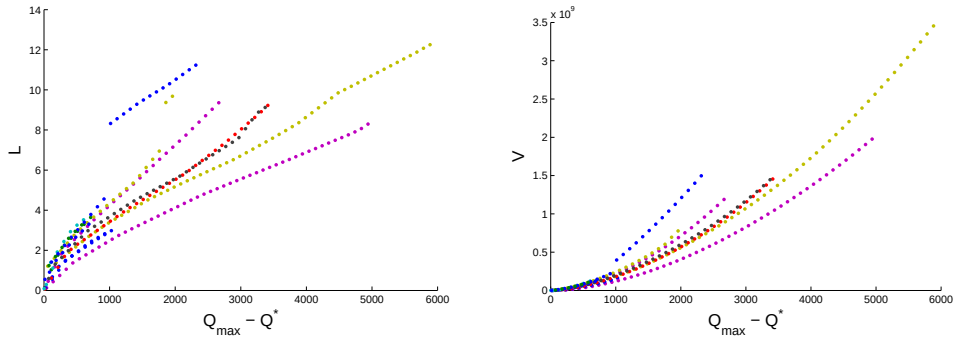

Figure 7: Left: Scatter plot of the length L of an interval in which the discharge Q is above a certain threshold Q^*. The values are given as a function of $\tilde{Q} = Q_{\max} - Q^*$. The aim is to draw conclusions that are independent of the peak height $Q_{\max}$. Data points corresponding to the same peak have the same colour. Right: Scatter plot of the volume V of water in a flood wave above a certain threshold Q^*. The values are given as a function of $\tilde{Q} = Q_{\max} - Q^*$. Data points corresponding to the same peak have the same colour.

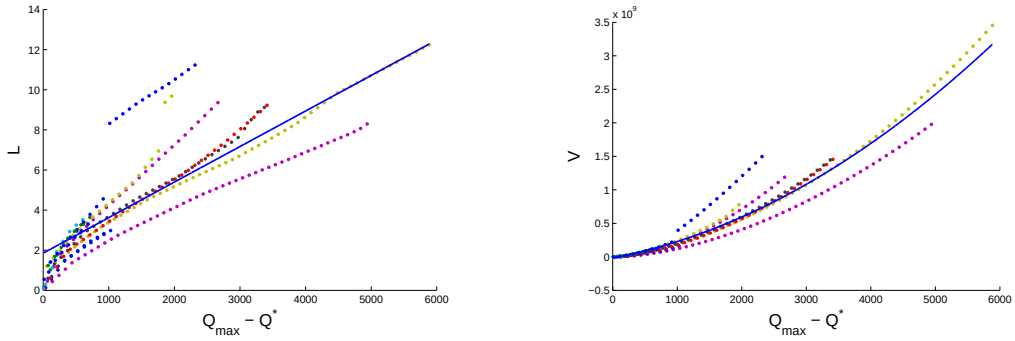

Figure 8: Left: A linear relation fitted to the data of Figure 7, left-hand side. Right: A parabolic relation fitted to the data of Figure 7, right-hand side. Note that slightly negative values occur in the graph due to the fitted parabola, not due to the data (cf. Figure 7, right-hand side).

There is more to criticize about these fitted relations. From a physical point of view it is clear that $L(\tilde{Q}) = 0$ and $V(\tilde{Q}) = 0$ should hold if $\tilde{Q} = 0$. This is clearly not the case in the fitted line in Figure 8, left. Moreover, (9) is violated. We have fitted:

$$L = a\,\tilde{Q} + b, \tag{10}$$

$$V = c\,\tilde{Q}^2 + d\,\tilde{Q} + f. \tag{11}$$

The fitted parameter values are

$$a = 0.0018, \tag{12}$$

$$b = 1.8533, \tag{13}$$

$$c = 60.7973, \tag{14}$$

$$d = 1.8422 \cdot 10^5, \tag{15}$$

$$f = -1.7661 \cdot 10^7. \tag{16}$$

It follows from (9) that $2c = \tau\, a$ and $d = \tau\, b$ should hold. The fitted coefficients satisfy

$$\frac{2c}{\tau\, a} = 0.7944, \tag{17}$$

$$\frac{d}{\tau\, b} = 1.1505, \tag{18}$$

which both do not really convince us that the above fits are appropriate.

In Figure 9 we show that using double logarithmic axes are of help here. The represented data is the same as in Figure 7.

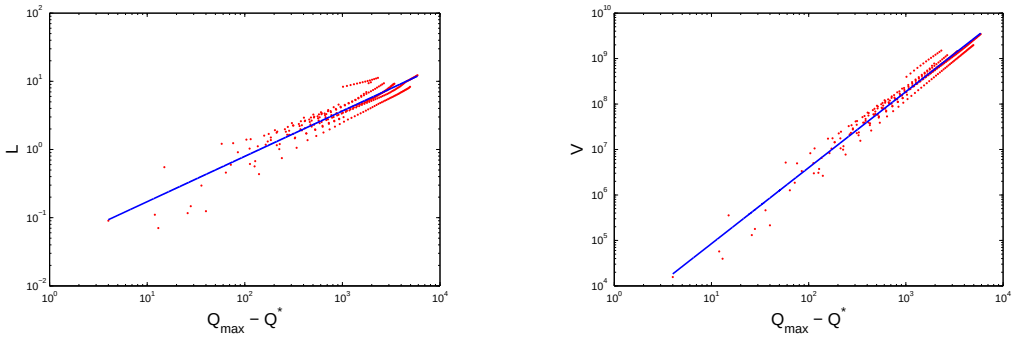

Figure 9: Left: The data of Figure 7, left, plotted in double logarithmic axes. A linear relation is added (i.e. linear in double logarithmic scaling). Right: The data of Figure 7, right, plotted in double logarithmic axes. A linear relation is added (i.e. linear in double logarithmic scaling).

In these axes the correlation between $\tilde{Q}$ on one hand and L or V on the other hand, is much clearer. To emphasize this, in both cases a linear fit is added. To show that these fits are much better than the previous ones, we add them to Figure 8, the result of which is shown in red in Figure 10. Especially, we see in Figure 10, left, that the issues that arose for the linear fit are resolved. Both for small and for large $Q_{\max} - Q^*$ the fit resembles the data. Moreover, these fits

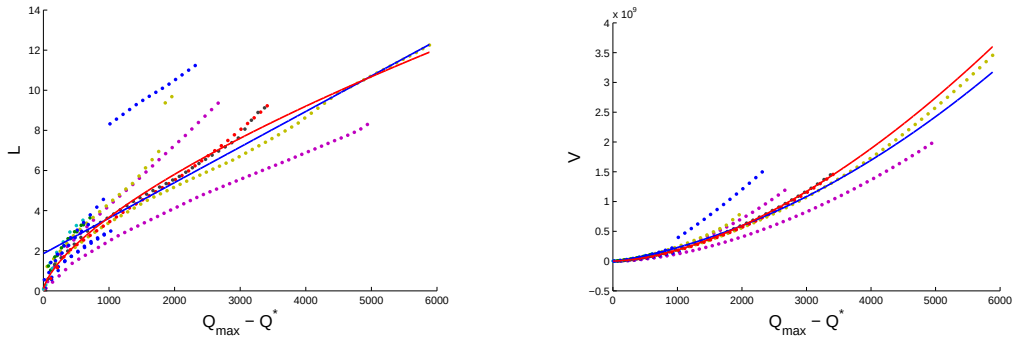

Figure 10: Left: The data of Figure 7, left, with fitted a linear relation (blue, cf. Figure 8, left) and an exponential relation (red, cf. Figure 9, left). Right: The data of Figure 7, right, with fitted a linear relation (blue, cf. Figure 8, right) and an exponential relation (red, cf. Figure 9, right).

pass the origin by definition. We have fitted

$$\log L = A\, \log \tilde{Q} + B, \tag{19}$$

$$\log V = C\, \log \tilde{Q} + D, \tag{20}$$

or, equivalently,

$$L = e^B \, \tilde{Q}^A, \tag{21}$$

$$V = e^D \, \tilde{Q}^C, \tag{22}$$

which are positive for positive $\tilde{Q}$. The fitted parameter values are

$$A = 0.6646, \tag{23}$$

$$B = -3.2929, \tag{24}$$

$$C = 1.6708, \tag{25}$$

$$D = 7.5011, \tag{26}$$

for which (9) implies that $C\,e^D = \tau\,e^B$ and $C - 1 = A$ should hold. The fitted coefficients satisfy

$$\frac{C\,e^D}{\tau\,e^B} = 0.9423, \tag{27}$$

$$\frac{C-1}{A} = 1.0093. \tag{28}$$

This is more satisfying than our earlier attempt. Note that comparing these numerical values quantitatively to (17)–(18) does not make sense, since the coefficients in (17)–(18) and (27)–(28) have different meanings.

We use the exponential fit to make some predictions about what to expect for $Q_{\max} = 18000$ m^3/s and $Q^* = 17500$ m^3/s. These numbers are the reference situation provided by *Rijkswaterstaat*. They serve as an illustration here, as similar computations can be made for other thresholds.

For $\tilde{Q} = 500$ m^3/s our fitted relations (21)–(22) predict the following values:

$$L = 2.3107 \text{ days}, \tag{29}$$

$$V = 5.8502 \cdot 10^7 \text{ m}^3. \tag{30}$$

This means that the outlet to the retention area needs to be opened roughly two and a half days, and that in total nearly 59 million m^3 needs to be stored. According to these predictions, the Rijnstrangen area (capacity: 150 million m^3) would be more than sufficient as a retention area.

Two remarks about these predictions need to be made:

1. No data is available for discharges as large as 18000 m^3/s. This is because these values are currently not reached, but they are expected in the future due to climate change. Our predictions are only based on historic data. Extrapolation to changing situations in the future therefore requires caution. A positive point is however that the data used does contain information about 23 annual extreme events (represented by $Q_{\max}$ values). By introducing the translated coordinate $\tilde{Q}$, we account for the fact that the value of $Q_{\max}$ is different every year. As a result, the predicted value at $\tilde{Q} \approx 500$ in some sense contains information from the whole data set.

2. Our fitted relations reflect more or less the average trend of the data. It might be of more interest to know about the extremes (e.g. extremely high $Q_{\max}$ and simultaneously rarely high $L(\tilde{Q})$). We wish to state explicitly that these cases are not treated here.

3.2.2 An alternative approach

There is also an alternative approach to which there are some disadvantages. These will be commented on later in this section. In fact these negative aspects drove us to the approach described in Section 3.2.1.

The alternative approach is based on the assumption that a peak can be approximated locally by a parabola.[1] If its maximum $Q_{\max}$ is attained at time t_0, then the discharge Q as a function of time t is assumed to be given by

$$Q = Q_{\max} - \frac{1}{2}\,\alpha\,(t - t_0)^2. \tag{31}$$

Note that

$$\frac{d^2Q}{dt^2} = -\alpha, \tag{32}$$

where α is a parameter still to be identified. The second derivative is (a measure for) the curvature of the graph at the peak. Again we have to be careful about the units here. The second derivative d^2Q/dt^2 should have the unit of volume/(time^3). Since Q is measured in m^3/s and t in days, the unit of d^2Q/dt^2 is m^3/(s $\cdot$ days^2). At first sight this might seem a bit artificial. In the sequel, we write Q'' instead of d^2Q/dt^2, keeping well in mind this issue about the units.

An encouraging observation in this approach is the following. There appears to be a correlation between the value of Q_{max} and the second derivative Q'' in that point. In short: higher peaks are more narrow. This is shown in Figure 11 where we plot a numerical (second-order) approximation of Q'' against $Q_{\max}$ for all local maxima from July 1989 to June 2012. A linear fit is added to emphasize the correlation. We use all local maxima, instead of just annual maxima, since our fit would otherwise depend on only 23 data points. From this fit we are able to extrapolate (e.g. to

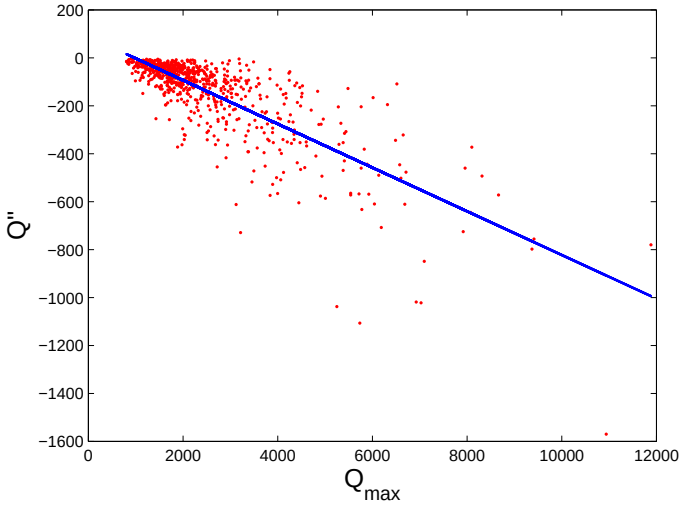

Figure 11: Scatter plot of the (numerical) second derivative in the top, against the discharge value in the top $Q_{\max}$. The linear correlation is indicated by the blue line. The units are: $[Q]$ = m^3/s, $[t]$ = days. To base the fit on a sufficiently large data set, all local maxima are used; not just the annual maxima.

$Q_{\max} = 18000$) and find the corresponding value for Q''. Moreover, exact calculations lead to the following expressions

$$L = \sqrt{2\frac{Q_{\max} - Q^*}{\alpha}}, \tag{33}$$

$$V = \frac{4}{3}\sqrt{\frac{2}{\alpha}}\,\tau\,(Q_{\max} - Q^*)^{3/2}, \tag{34}$$

[1] This is a strong assumption, but still the results turn out to be useful.

for the interval length L and volume V, respectively. From these expressions predictions for L and V are easily made, once we provide e.g. $Q_{\max} = 18000$ m^3/s, $Q^* = 17500$ m^3/s and the extrapolated value of $Q'' = -\alpha$. We find:

$$L = 0.8028 \text{ days}, \tag{35}$$

$$V = 4.6241 \cdot 10^7 \text{ m}^3. \tag{36}$$

These predictions imply that Rijnstrangen area (capacity: 150 million m^3) is sufficiently large to contain the amount of water that needs to be stored. Compared to the prediction of Section 3.2.1, the value of L is very low.

The latter statement about L indicates that we should be cautious here. In Figure 12 we have a closer look at the quality of the fits provided by (34). We can see that sometimes (e.g. for 27 March 2001) the fit very poorly represents the actual data. For other peaks (e.g. 17 February 2005) the fit is appropriate. We emphasize that we should concentrate on the error for relatively

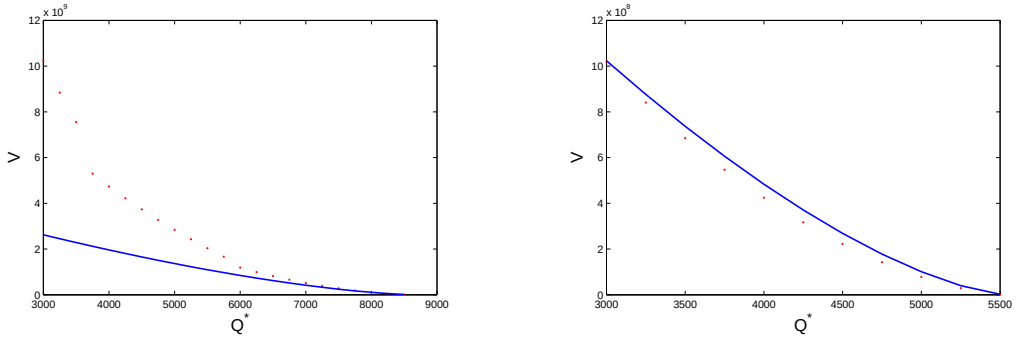

Figure 12: Left: Data, in red, and fit (34), in blue, for V corresponding to the annual maximum discharge which was attained on 27 March 2001. The fit deviates significantly from the data. Right: Data, in red, and fit (34), in blue, for V corresponding to the annual maximum discharge which was attained on 17 February 2005. The fit agrees quite well with the data.

small $\tilde{Q}$, since $\tilde{Q} = 500$ is the reference situation. Figure 12 strongly suggests to have a closer look at how well the approximations (33)–(34) perform, and especially for $\tilde{Q} \approx 500$.

Let L_{m} and V_{m} denote the actual *measured* quantities. The quantities fitted according to (33)–(34) are L_{f} and V_{f}. We consider the relative errors $|L_{\text{m}} - L_{\text{f}}|/L_{\text{f}}$ and $|V_{\text{m}} - V_{\text{f}}|/V_{\text{f}}$ in Figure 13. Intentionally, only relatively small $\tilde{Q} = Q_{\max} - Q^*$ are shown, since our predictions are for $\tilde{Q} = 500$. In the graphs we see no particular trend, but it is important to note that the order of magnitude of the error in L is 3.5 and of the error in V is 0.9. We wish to use these estimates for the error to improve our predictions (35)–(36). Note that if e.g. $|L_{\text{m}} - L_{\text{f}}|/L_{\text{f}} < \beta$, then $L_{\text{m}} < (1+\beta)L_{\text{f}}$. By multiplying our predictions by "$1 + \mathcal{O}(\text{error})$" we thus get an upper bound for the quantity we want to predict.
We multiply the predictions in this case by $1 + 3.5 = 4.5$ and $1 + 0.9 = 1.9$, respectively. What we obtain are the improved predictions:

$$L = 3.6126 \text{ days}, \tag{37}$$

$$V = 8.7859 \cdot 10^7 \text{ m}^3. \tag{38}$$

Note that these values still imply that the retention area is large enough.

For comparison, we also show the error plots for the approach of Section 3.2.1. The relative errors of L and V are given in Figure 14. An important point is that there is a trend. The relative error decreases for increasing $\tilde{Q}$ as indicated by the blue dashed line (which estimates the maximum error). It levels off to approximately 0.5 for L and 0.6 for V.

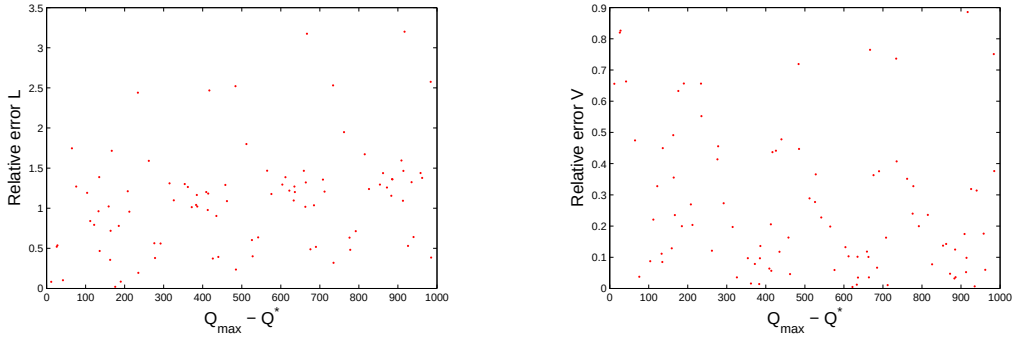

Figure 13: Left: Relative error in the prediction (33) of L, compared to the actual data, as a function of $\tilde{Q}$. Right: Relative error in the prediction (34) of V, compared to the actual data, as a function of $\tilde{Q}$.

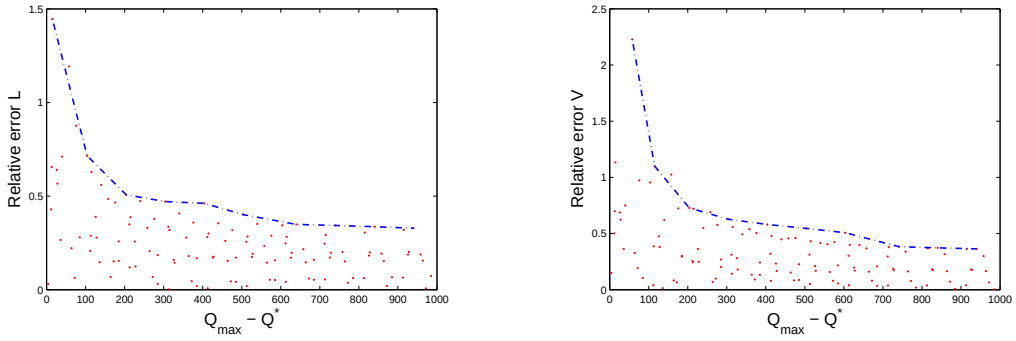

Figure 14: Left: Relative error in the prediction (21) of L, compared to the actual data, as a function of $\tilde{Q}$. The blue dashed line is an indication of the maximum error. Right: Relative error in the prediction (22) of V, compared to the actual data, as a function of $\tilde{Q}$. The blue dashed line is an indication of the maximum error.

Again, we use these estimates of the relative error to improve our predictions. We thus multiply (29)–(30) by 1.5 and 1.6, respectively. Our new predictions are

$$L = 3.4661 \text{ days}, \tag{39}$$

$$V = 9.3603 \cdot 10^7 \text{ m}^3. \tag{40}$$

We remark that the predictions for L are, after correction, more in agreement: compare (37) and (39). Moreover, the improved prediction (40) remains lower than the capacity of the Rijnstrangen area.

3.3 Summary

We summarize the results of Section 3:

- The annual maxima of our data set obey a Type I extreme value distribution (or: Gumbel distribution), whose parameters are $\mu = 5965.3$ m^3/s and $\sigma = 1625.4$ m^3/s; cf. (5). Knowing this distribution we can e.g. estimate that $\mathbb{P}(Q > 17500) = 8.2763 \cdot 10^{-4}$; cf. (6).
- According to the aforementioned distribution, statistically, once every 1250 years a discharge level of 17 555 m^3/s will be exceeded; see Section 3.1.2.

- We expect a peak with maximum discharge 18000 m^3/s to remain above the level of 17500 m^3/s for about three and a half days. In this prediction we have taken into account a correction for the error in our approximation; see (39) and (37). The capacity of the Rijnstrangen area is large enough to contain the excess of water if we open the outlet at $Q^* = 17500$ m^3/s and a maximum discharge of 18000 m^3/s is eventually attained; cf. (40) and (38).

The following remarks need to be made:

- Our predictions and claims are based on data, and as such describe the current situation. We are not able to account for future changes in climate and the consequences thereof.
- The fitted probability distributions and relations between quantities more or less describe the *typical behaviour* of extreme events. One could imagine that, given the fact that a certain peak discharge has an extreme value $Q_{\max}$, its other characteristics (like duration L) are also variable. Our claims are then about the average duration of the extreme event, and we do not have information about the distribution of L (i.e. the conditional distribution, given the maximum value $Q_{\max}$) or its dispersion. Thus, we cannot predict anything about how probable it is (for example) that such extreme event also lasts extremely long.
- We have shown that the retention area will have to be used only very rarely. Having two such events one shortly after the other is therefore (even more) unlikely to occur. From this point of view, there is no need for emptying Rijnstrangen very quickly after inundation, in order to be able to use it again. We do not address the issue of emptying in this report. However, due to the above arguments we believe that it is a minor factor in the overall decision process. Of course, we understand there might be other reasons (social, economic, geological,...), but these are beyond the scope of the present study.

4 Rhine system discharge model

One option to be considered for peak discharge retention relies on static weirs installed in the winter dikes that permit runoff of extreme discharge peaks into the Rijnstrangen region. Because the height of these weirs is only a few centimeters lower than the channel free surface height at extreme flood level, and to attain the desired retention rate of $\Delta Q = 500 m^3/s$, the static weirs must extend over several kilometers atop the winter dike. For the design of the weirs we must estimate the extreme flood level free surface height in the Rhine within the model region. To this end we construct a 1D hydrological model in this section. The spatial domain of the model consists of a 35 km section of channel beginning 5 km upstream from Lobith and extending along the Upper Rhine, Pannerdens Canal and IJssel. The bifurcations at the Waal and Lower Rhine are modeled as geometric discontinuities at which outflow occurs.

Denote by x the distance downstream from Lobith, $x \in [x_0, x_0 + L]$, where $x_0 = -5$km (location of the German border) and $L = 35$km. The channel is assumed to have vertical walls with width given by $w(x)$, which is a piecewise continuous function with jump discontinuities at bifurcation points x_A and x_B. The free surface height $h(x,t)$ is defined with respect to a mean bottom orography. The fluid model is given by the St. Venant or shallow water equations for flow in a channel

$$wh_t = -(whv)_x + q, \tag{41}$$

$$v_t = -vv_x - gh_x + g(S - S_f), \tag{42}$$

where $v(x,t)$ is the mean cross-sectional velocity, $q(x,t)$ represents the lateral inflow per unit length (i.e. negative for outflow over a weir), g is the gravitational acceleration, $S(x)$ is the slope of the bottom, and $S_f(x)$ is the friction slope, which encodes the combined forces of friction. For future reference we also introduce the cross-sectional flow area $A(x,t) = h(x,t)w(x)$

The St. Venant equations can be simplified using scaling assumptions [1]. The most appropriate of these are the kinematic wave approximation, for which the momentum equation (42) is replaced by the balance relation

$$S_f = S, \tag{43}$$

and the diffusion wave approximation in which (42) is replaced by

$$S_f = S - h_x. \tag{44}$$

The friction slope is defined as

$$S_f = \frac{n^2}{k^2}\frac{Q^2}{A^2 R_h^{4/3}}, \tag{45}$$

where $k = 1$ for SI units, n is the Gauckler-Manning coefficient, $Q = Av = hwv$ is the flow rate, and R_h is the hydraulic radius:

$$R_h = \frac{hw}{w + 2h} \approx h$$

These equation express a depth-averaged flow in a thin, incompressible fluid layer [1]. Inserting (45) in (43) and solving for v yields the flow speed

$$v = \frac{1}{n}h^{2/3}S^{1/2}, \tag{46}$$

from whence the kinematic wave model is reduced to

$$wh_t = -(\kappa(x)w(x)h^{5/3})_x + q, \tag{47}$$

where $\kappa(x) = S(x)^{1/2}/n(x)$. The Gauckler-Manning coefficient has been estimated for flow over surfaces of different roughnesses. We take $n(x) \equiv 0.03$ uniformly here.

Similarly, the diffusion wave approximation (44) can be solved for v to yield

$$v = \frac{1}{n}h^{2/3}(S - h_x)^{1/2} \approx \frac{1}{n}h^{2/3}(S^{1/2} - \frac{1}{2}S^{-1/2}h_x),$$

which in turn gives a nonlinear advection-diffusion equation for h.

The kinematic wave model (47) assumes the form of a hyperbolic conservation law for the height $h(x,t)$. To specify a unique solution, it must be equipped with appropriate initial and boundary conditions. We will assume that all characteristics are monotone in the downstream direction, meaning that it is only necessary to specify the inflow at the upstream boundary. Given an inflow discharge $Q_0 = Q(x_0, t)$, we can determine the inflow layer depth $h_0(t)$ from

$$h_0 v_0 = \frac{Q_0}{w(x_0)}$$

by substituting (46) in the above expression and solving for h_0. An initial condition can be obtained by solving

$$-(\kappa(x)w(x)h^{5/3})_x = 0$$

with this initial condition:

$$h(x,0) = h_0(0) - \int_{x_0}^{x} \kappa(s)w(s)h(s)^{5/3}\,ds.$$

Numerically, one can simply choose a constant layer depth $h(x,0) = h_0(0)$ and solve with constant inflow until steady state is reached.

Note that the velocity in the Rhine system is on the order of 1 m/s. This means that any given fluid parcel passes out of the system within about 8 hours. If variations in the inflow $h_0(t)$ are slow on this time scale, then the system is quasi-steady state, with height given by the previous expression. In this case too, the differences between the kinematic wave and diffusive wave models will be small.

5 Numerical unsteady flow computation

In this section we present a simple numerical code to solve the 1D model developed in the previous section, with the goals of (1) providing a tool that can be used for studying more complex retention scenarios, such as the placement of outlets at strategically chosen points around Rijnstrangen (not considered in this report), and (2) to show that for the flooding scenario predicted in §3, with excess peak discharge lasting more than 72 hours, the flow can be assumed to be in quasi-equilibrium state. At the end of the section, two computational scenarios reflecting these goals, are included, the first illustrating that the code can be used for transient calculations if so desired, and the second illustrating that even for a flooding scenario lasting < 48 hours, quasi-equilibrium is a good approximation.

Since our model includes only that part of the total discharge that flows through the trajectory Upper Rhine, Pannerdens Canal, IJssel, it is crucial for the numerical model to properly treat the outflows into the Waal and Lower Rhine, to avoid reflected waves or other numerical artifacts. We consider a class of finite volume methods with the necessary properties. We define grid points $x_i = x_0 + i\Delta x$, $i = 0, \ldots, N$, $N\Delta x = L$. The channel width at grid point i is denoted w_i. We allow the width to change discontinuously at a grid point, and denote the upstream and downstream values by w_i^- and w_i^+, respectively. The bottom slope S_i and the Gauckler-Manning coefficient n_i are also specified at grid points. The outflow per unit length q is approximated at the midpoint of the interval $q_{i+1/2} \approx q(x_{i+1/2})$.

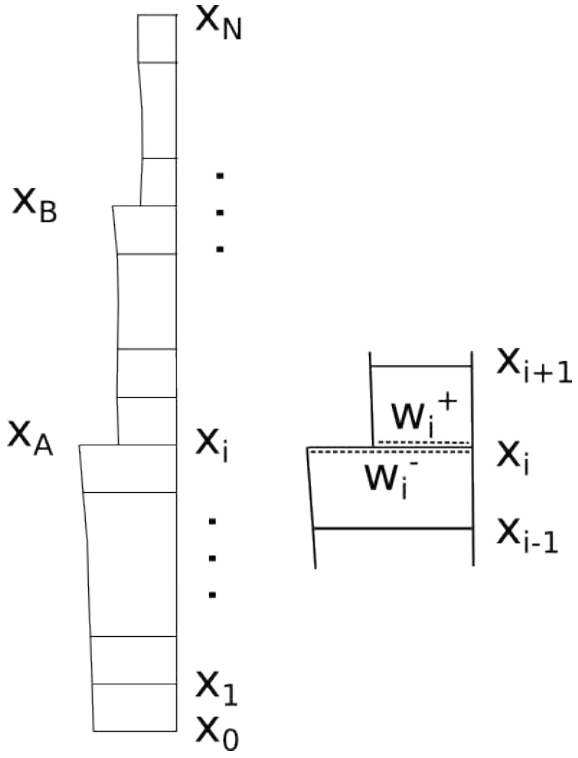

Figure 15: Discrete geometry. Left: one-dimensional grid in x, with channel widths w_i specified at grid points x_i and indicating discontinuities at bifurcation points x_A and x_B. These are the points A and B indicated in Figure 1. Right: a discontinuity in channel width w_i at grid point x_i, modelling outflow at a bifurcation.

To determine the layer depth $h_i(t)$ at grid point i, we discretize (47) using a compact one-parameter class of finite volume schemes. This class of discretizations has the property that it preserves the dispersion relation of the underlying PDE, in the sense that sign of group velocity is always correct.

This means that information always flows downstream when it should, allowing us to model outflow at bifurcation points and at the end of the domain without incurring numerical side effects like reflected waves. The discretization is defined for a generic grid interval (x_i, x_{i+1}):

$$\theta w_i^+ \frac{\partial h_i}{\partial t} + (1-\theta) w_{i+1}^- \frac{\partial h_{i+1}}{\partial t} = -\frac{1}{\Delta x}(Q_{i+1}^- - Q_i^+) + q_{i+1/2}, \tag{48}$$

where the discrete fluxes are defined by

$$Q_i^\pm = \frac{S_i^{1/2}}{n_i} w_i^\pm h_i^{5/3}.$$

The parameter θ may take values in $(0, 1/2)$. For $\theta > 1/2$ the scheme is unstable for flow in the positive x direction. The scheme is implicit for $\theta > 0$ due to the weighted average on the left side. The choice $\theta = 0$ corresponds to upwind differencing, which is first order accurate, monotone, and highly diffusive. The choice $\theta = 1/2$, which is symmetric and the only second order choice, yields the Preissman box scheme, well known in hydrology. However it is implicit, so for efficiency we have only implemented the case $\theta = 0$ here.

It can be checked by summing both sides of (48) that total mass $\sum_i h_i w_i$ is conserved locally when there is no inflow or outflow ($q_{i+1/2} = 0$, $w_i^+ = w_i^-$, for all i).

To model a bifurcation (points A and B in Figures 1 and 15), we choose the grid point closest to the bifurcation point, say x_i. Define w_i^- to be the width of the channel directly upstream of the bifurcation, and w_i^+ to be the width of the branch whose flow is to be included in the model. Let $w_i^{\text{out}} = w_i^+ - w_i^-$, then balance of flux at x_i requires $Q_i^- = Q_i^+ + Q_i^{\text{out}}$. Hence a specific outflow-to-inflow ratio requires

$$\gamma = \frac{Q_i^{\text{out}}}{Q_i^-} = \frac{Q_i^- - Q_i^+}{Q_i^-} = 1 - \frac{w_i^+}{w_i^-} = \frac{w_i^{\text{out}}}{w_i^-}.$$

Consequently a discontinuous change in channel width of ratio γ yields a corresponding change in discharge of ratio γ.

For $\theta = 1/2$ it is recommended to integrate (48) in time with the implicit midpoint rule. In this paper, we choose $\theta = 0$ and integrate in time with the well-known fourth order explicit Runge-Kutta method.

It is a straightforward matter to adapt the 1D Matlab code, given accurate geometrical channel data from the Upper Rhine region, as well as discharge data for Lobith. During the Study Group Week, a geometrically simple scenario was computed, using uniform channel widths between each bifurcation point, with the widths chosen to achieve the correct relative discharge rates in each branch of channel model.

We take domain parameters $x_0 = -5$km (German border) and $L = 35$km, such that Lobith is at $x = 0$. Moreover, we take $\Delta x = 100$m and uniform canal segments of width $w_0 = 1500$m in the Upper Rhine, dropping discontinuously to $0.36w_0$ at the Pannerdens Canal bifurcation point and to $0.15w_0$ at the IJssel bifurcation point. We assume uniform values of $n = 0.03$ and $S = 1 \times 10^{-4}$. In all simulations, the time step was taken to be $\Delta t = 50$s, and the initial condition was taken to be a stationary flow with discharge at Lobith corresponding to 5000 m^3/s.

We considered two flooding scenarios, based on the current peak discharge design capacity of 16000 m^3/s and the proposed new design capacity of 17500 m^3/s. In both cases a Gaussian (in time) discharge profile was defined with peak flow rate $Q_{\max} = 18000$ m^3/s. It is assumed that all discharge exceeding the design capacity is removed instantly at Lobith ($x = 0$), meaning the inflow profiles are capped at 16000 and 17500 m^3/s, respectively. In the first scenario, the peak was attained in 2 days to illustrate transient effects. In the second scenario the peak was reached in 11.5 days.

Figure 16 illustrates the results for the transient case with design discharge capacity 16000 m^3/s. We observe a rapid increase in flow rate, especially in the Upper Rhine segment, at 30 and 40 hours, but a steady state has been reached at the peak flow after 50 hours. The total retention in the Rijnstrangen area is between 60 and 70 million cubic meters.

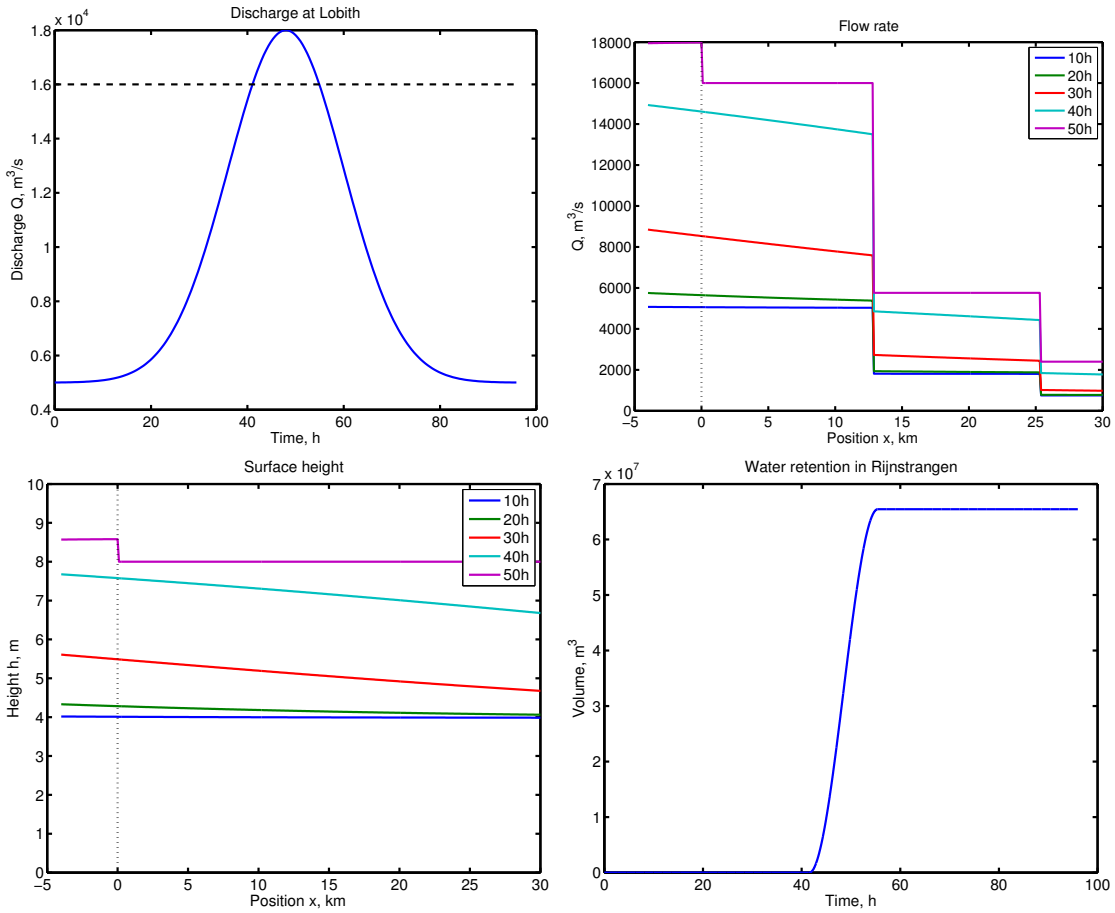

Figure 16: Flooding scenario reaching 18000 m^3/s in 2 days at current design peak discharge of 16000 m^3/s. Top left: discharge scenario at Lobith. Top right: flowrates throughout the domain at sequential times; discontinuities occur at channel bifurcation points. Bottom left: free surface height in the domain at sequential times; discontinuity at $x = 0$ due to removal to Rijnstrangen retention area. Bottom right: volume of water retained in Rijnstrangen area as a function of time.

Figure 17 illustrates the results for the longer event with peak after 11.5 days. In this case the flow may be assumed to be quasi-steady state, with the levels being nearly stationary at any given time. For the proposed design discharge capacity of 17500 m^3/s, the required retention in the Rijnstrangen area is 45 million cubic meters.

We stress that these computations are illustrative only! An accurate computation of transient flow would require correct measurements of the outer dike geometry. Furthermore the effects of sloping dike walls and the inner dike geometry have been neglected in the model. In general, the bottom slope $S(x)$ and Gauckler-Manning coefficient $n(x)$ should be properly estimated, and generally vary in x. Finally, the precise transient dynamics depend on the inflow discharge profile $Q_0(t)$ and Rijnstrangen outlet configurations.

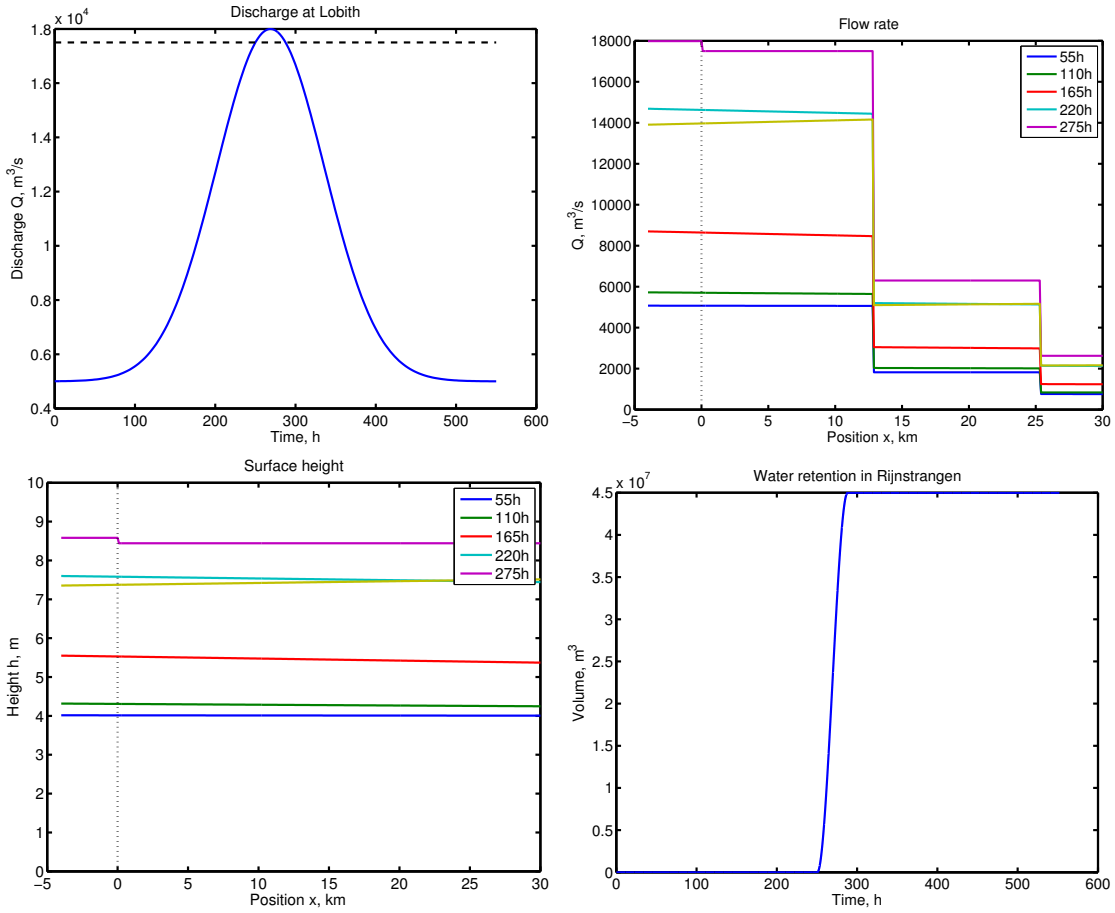

Figure 17: Flooding scenario reaching 18000 m^3/s in 11.5 days at proposed design peak discharge of 17500 m^3/s. Top left: discharge scenario at Lobith. Top right: flowrates throughout the domain at sequential times; discontinuities occur at channel bifurcation points. Bottom left: free surface height in the domain at sequential times; discontinuity at $x = 0$ due to removal to Rijnstrangen retention area. Bottom right: volume of water retained in Rijnstrangen area as a function of time.

6 Outlet configurations

We restrict ourselves to a single outlet before the first bifurcation of the river Rhine. The advantage is that a single outlet could suffice, while this would not be possible for an outlet after the first bifurcation without affecting the discharge ratio at the first bifurcation. For this case the following values for the discharge are relevant.

Let Q_{before} and Q_{after} denote the discharge of the river before and after the outlet. Also let Q_{outlet} be the discharge through the outlet so that the following conservation law holds: $Q_{\text{after}} + Q_{\text{outlet}} = Q_{\text{before}}$. To prevent flooding downstream it is required that $Q_{\text{after}} \leq 17500$. Here Q is measured in units of m^3/s, as in the rest of this section. Unnecessary use of the retention area comes at a high cost and may also limit uptake in the near future, so the preferred outlet has the property that:

$$Q_{\text{after}} = \min(Q_{\text{before}}, 17500). \tag{49}$$

We analyse several ideas for constructions of the outlet to the reservoir. After introducing our simple model we first study the construction of a weir, where water flows over the weir into the reservoir. A weir is a passive construction: water only flows if it has reached a critical level.

Second we study the construction of a floodgate, by which we mean that a gate has to be lowered to reach the required outflow of water. In both cases, we investigate which size the outlet should have. Third we study an outlet where the water flows underneath a floodgate or through a pipe near the bottom of the river. Our analysis leads to estimates on the size of the constructions involved and gives insight into various other characteristics that need to be taken into account. These are all collected in the discussion at the end of this section.

6.1 A model for the flow of water over a weir

To calculate the flow over a weir, we use a so-called 'dam-break' model from [3, Section 10.5]. In this model the one-dimensional flow of water due to pressure is calculated on each location $x \in \mathbb{R}$ at time $t \geq 0$, where we assume the initial condition in Figure 18. That is, we assume that a dam is instantaneously removed at $x = 0$ and time $t = 0$ and water starts flowing from right to left.

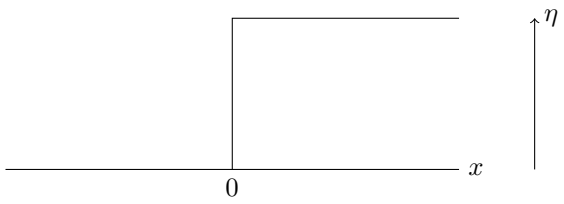

Figure 18: The initial condition at $t = 0$ in the dam-break model. The initial height of the water along the x-axis is denoted by η.

In [3, Section 10.5] an analytical solution is found using the method of characteristics. The model only depends on the initial height of the water above the weir, which we denote by η. The height of the water as a function of x at some time t is sketched in Figure 19. It turns out that the height η_0 at $x = 0$ is constant for all time $t > 0$ and is given by $\eta_0 = \frac{4}{9}\eta$. The velocity of the water u at $x = 0$ is also constant (over time and height) and is given by

$$u = \frac{2}{3}\sqrt{g\eta}, \tag{50}$$

where g is the gravitational constant. So the flux through $x = 0$ is

$$q = u\eta_0 = \left(\frac{2}{3}\right)^3 \sqrt{g}\eta^{\frac{3}{2}}.$$

We obtain the total flow over the weir Q_{outlet} by multiplying with the length of the weir, which we denote by l:

$$Q_{\text{outlet}} = \left(\frac{2}{3}\right)^3 \sqrt{g}\eta^{\frac{3}{2}} l. \tag{51}$$

We now apply this model to the situation where a weir is built alongside a river. We take a cross-section of the river and assume that this section moves with the velocity of the river, see Figure 20. If this cross-section arrives at the weir, then—from the perspective of the cross-section—the dike is instantaneously lower, and we apply the dam-break model.

If we denote the height of the weir by d, then the initial height of the water in the river is $h = d+\eta$. This situation is sketched in Figure 21. The x-axis in Figure 21 corresponds to the x-axis in Figures 18, 19 and 20. We take the weir to be flat in both the x-direction and the direction of the river flow. We neglect the effects of water in the river deeper than the top of the weir. We also neglect any effects resulting from the flow of water perpendicular to the cross-section (e.g. in the direction of the flow of the river).

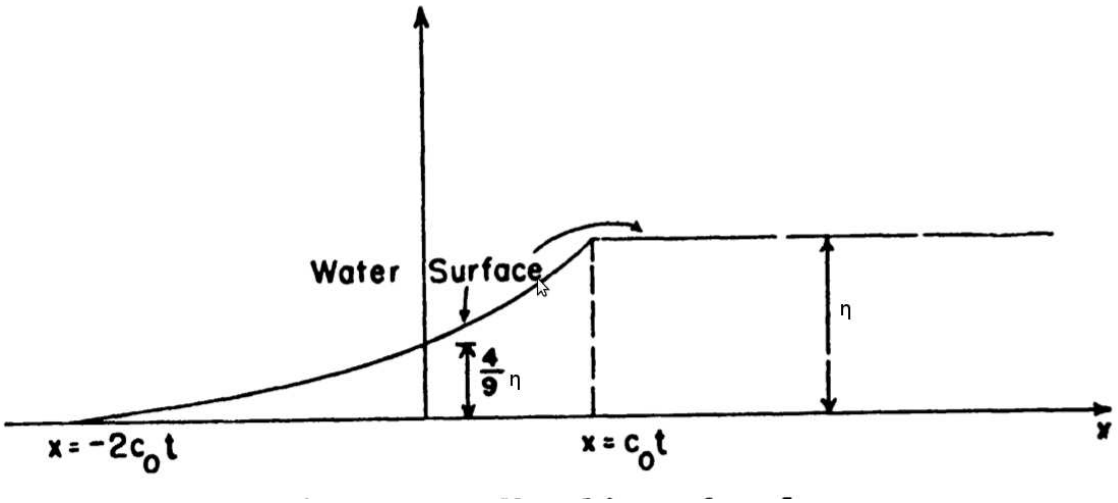

Figure 19: Dam-break model: the height of the water is sketched against the one-dimensional spatial variable x at time t. This figure is from [3, page 313], with adjusted variables.

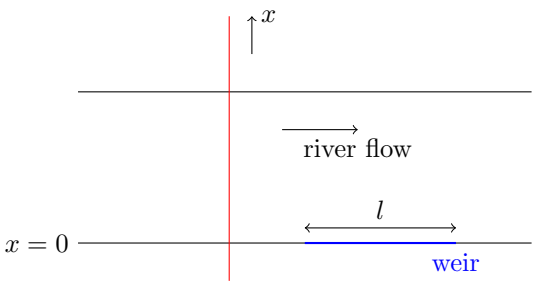

Figure 20: Depiction of the river from above with the cross-section (red) mentioned and the weir (blue). With this perspective we argue that we can apply the dam-break model.

Since d is fixed, the model depends on the height of the water in the river h which we obtain from the model derived in Section 4:

$$h = \left(\frac{nQ}{w\sqrt{S}} \right)^{\frac{3}{5}}, \tag{52}$$

where n is a constant depending on the river bed, Q is the discharge of the river (the flux in m^3/s), w is the width of the river and s is the slope of the river.

It follows from (51) that the power law $Q_{\text{outlet}} \propto \eta^{\frac{3}{2}}$ holds with proportionality constant $\left(\frac{2}{3}\right)^3 \sqrt{g}l$. In hydrology this power law is well-established. For instance in [4] section 5.1 the same power law is acquired from rough estimates for water flowing over a weir like in Figure 21. Assuming subcritical (laminar) flow before and supercritical (turbulent) flow after the weir, it is reasoned that at the weir the flow must be critical. Applying Bernoulli's principle (see equation (56) below) yields the same power law (but with a different proportionality constant).

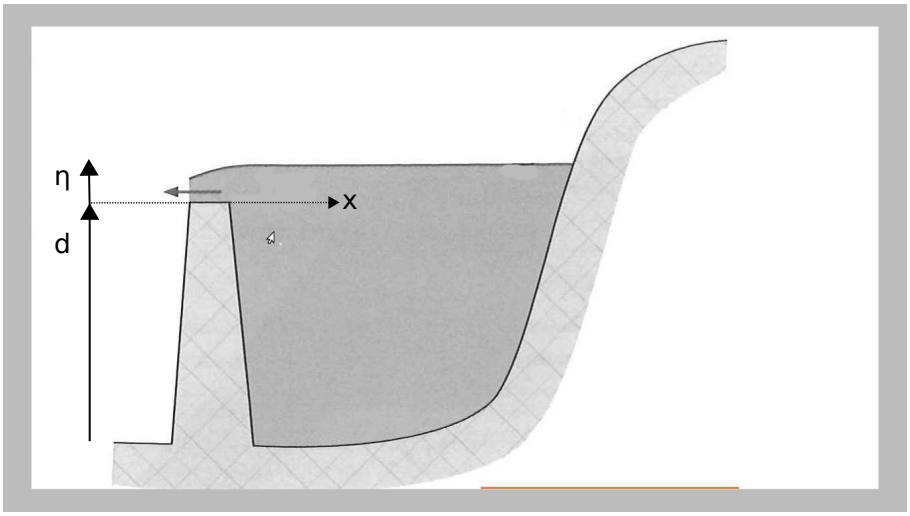

Figure 21: Cross-section of the river, with indication of the variables used. We assume the slope of the weir to be horizontal, so in contrast to what the picture suggests, the top of the weir continues to the left following the dotted line. This figure is from [4].

6.2 Constructions with water flowing over a weir

We first consider the situation of water flowing over a weir where d is constant over the length l of the weir. A weir with length l is constructed with a fixed height d, such that:

$$Q_{\text{outlet}} = 0, \text{ if } Q_{\text{before}} = 17500, \qquad \text{and} \qquad Q_{\text{outlet}} = 500, \text{ if } Q_{\text{before}} = 18000. \tag{53}$$

This weir is in essence a place where the dike is lowered, see also Figure 20 and Figure 21. We also require that water starts flowing over the weir only when $Q_{\text{before}} > 17500$ and investigate the implications of this requirement.[2].

The height d can be explicitly calculated from (52) and the first part of (53). It follows that the weir should be 7.10m. When $Q_{\text{before}} = 18000$, the height of the water level is $h = 7.22$m by (52). Consequently, we know the height of the water above the weir: $\eta = h - d$. Using (51) we can determine the length of the weir from the second part of (53). It follows that the weir has to be approximately 13 kilometers long. This is a disadvantage since there is no place in the Netherlands where it is possible to construct such a long outlet.

[2]This assumption ensures that the weir is no longer (and thus higher) than necessary.

Suppose that there would be an area long enough for this weir, then there is another disadvantage. One requirement of *Rijkswaterstaat* is that Q_{after} has to remain be below 17500 to avoid flooding downstream. From (52) and (51) an expression can be given of Q_{after} as a function of Q_{before} by:

$$\begin{aligned} Q_{\text{after}} =& Q_{\text{before}} - Q_{\text{outlet}} \\ =& Q_{\text{before}} - \left(\frac{2}{3}\right)^3 \sqrt{g} \left(\left(\frac{n Q_{\text{before}}}{\sqrt{S} w} \right)^{\frac{3}{5}} - d \right)^{\frac{3}{2}} l. \end{aligned} \tag{54}$$

In Figure 22, this function is plotted in blue for $Q_{\text{before}} \geq 17500$ (for $Q_{\text{before}} < 17500$, Q_{after} coincides with the black line.) The figure shows that this passive construction does not satisfy the condition of *Rijkswaterstaat* for intermediate values.

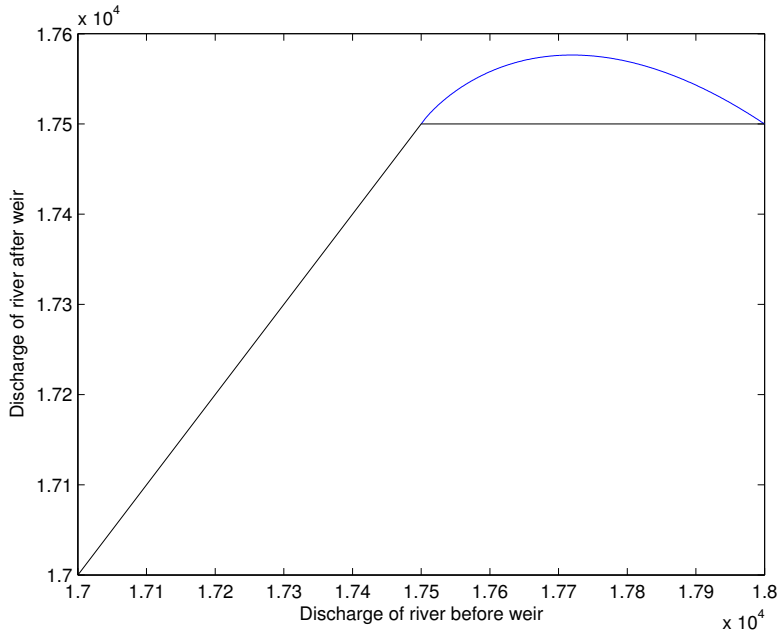

Figure 22: The discharge after the weir is plotted in blue against the discharge before the weir when using a weir of 13 kilometers long. The black line refers to the preferred situation (49). The requirement from *Rijkswaterstaat* that the discharge be reduced to $Q_{\text{after}} \leq 17500$, is not met.

To avoid the unwanted behavior at intermediate values of the previous weir we now replace one of the conditions of (53) by an equation on the derivative:

$$\frac{dQ_{\text{outlet}}}{dQ_{\text{before}}} = 1, \text{ if } Q_{\text{before}} = 18000, \qquad \textit{and} \qquad Q_{\text{outlet}} = 500, \text{ if } Q_{\text{before}} = 18000. \tag{55}$$

Because of the apparent concavity of (54) the condition on the derivative will preclude $Q_{\text{after}} \geq 17500$ and it will also minimize the amount of unnecessary water entering the retention area for these kinds of weirs. Again employing (52) and (51) with (55) leads to a relation which can be numerically solved for l and d, $l \approx 7$ kilometer and $d \approx 7.04$m. In Figure 23, Q_{after} is plotted against Q_{before}, with the formula in (54). The figure shows that Q_{after} never exceeds 17500, but it also shows that from $Q_{\text{before}} = 17250$ onward, there is already water flowing over the weir. But the superfluous amount of water entering the retention area stays below 100 m^3/s all the time.

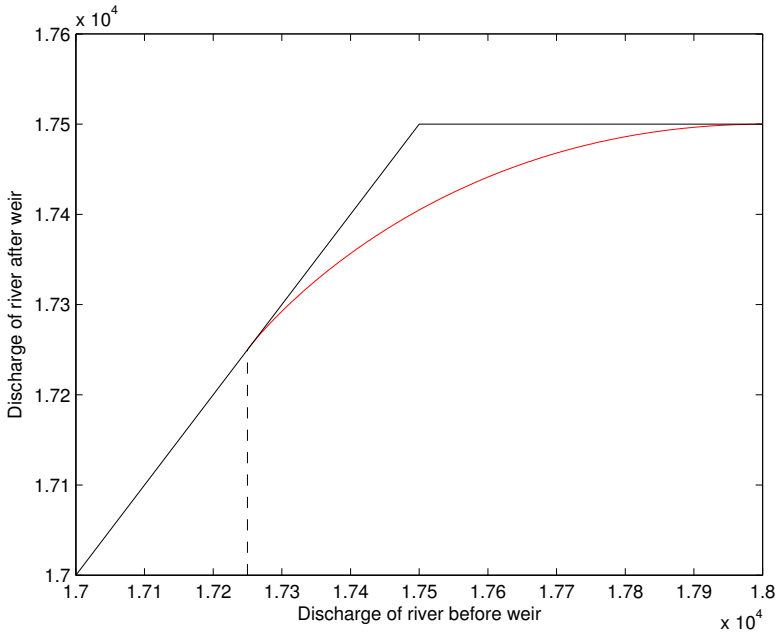

Figure 23: The red curve indicates the discharge after the weir when a weir construction is used, with a length of 7 km. The black line again refers to the preferred situation in (49). The condition $Q_{\text{after}} \leq 17500$ holds for all values of Q_{before}, but water starts flowing into the retention area already at $Q_{\text{before}} = 17250$, indicated with the dashed line.

6.3 Constructions with water flowing over a floodgate

As we saw in the previous section passive constructions need to be very long. In this section we look at controllable floodgates; essentially these are weirs of variable height. So water is assumed to flow over the floodgate, this allows us to use the dam-break formulas derived previously.

First we consider a floodgate whose height can be continuously adjusted to allow for precisely the correct amount of water entering the retention area. We give a description of how this height needs to be adjusted. Second we look at a floodgate which can be either open or closed.

6.3.1 Continuous control

The preferred outlet (49) for $Q_{\text{before}} \geq 17500$ is equivalent to $Q_{\text{outlet}} = Q_{\text{before}} - 17500$. Using this, (51), (52) and $\eta = h - d$ we obtain an equation for the height of the floodgate as a function of Q_{before} and l:

$$d = \left(\frac{nQ_{\text{before}}}{\sqrt{S}w}\right)^{\frac{3}{5}} - \frac{9}{4}\left(\frac{Q_{\text{before}} - 17500}{\sqrt{g}l}\right)^{\frac{2}{3}}.$$

For several choices of l we have plotted the graph in Figure 24.

In theory it is now easy to build the preferred outlet. But implementation may be complicated as the height needs to be continuously adjusted and calculated from a known discharge. This relatively complicated procedure may be prone to errors and since high discharge is assumed to be a rare event it may be hard to tune the floodgate correctly.

To partially circumvent these problems we next look at a floodgate that can either be open or closed.

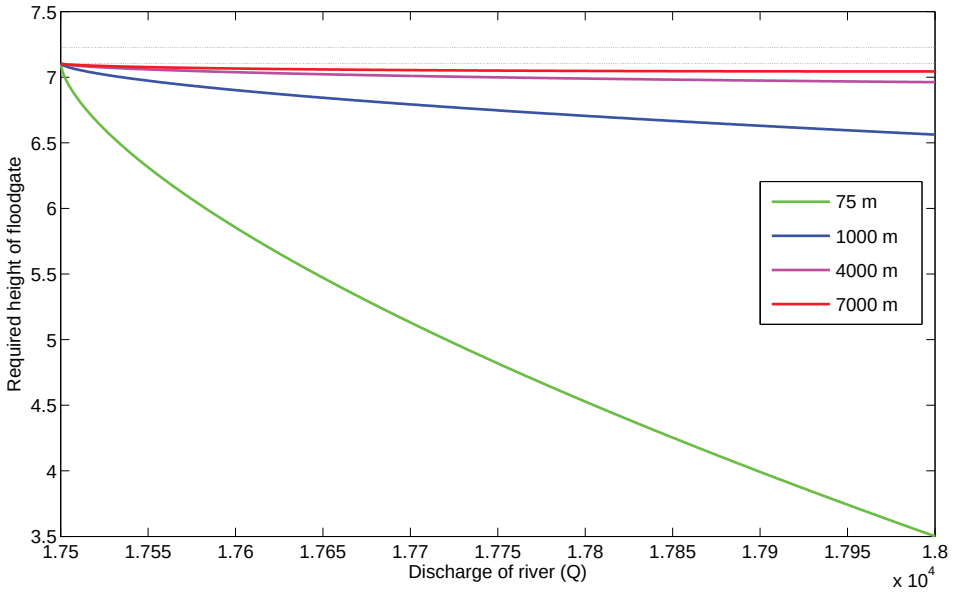

Figure 24: Height of floodgate in meters above the bottom of the river to reduce Q_{after} to 17500. Smaller floodgates (in length) need to be lowered more to allow enough flow through. When floodgates are controlled accordingly, each floodgate has the preferred property (49). The dotted horizontal lines at height 7.10 and 7.22 are the heights of the river at $Q_{\text{before}} = 17500$ resp. $Q_{\text{before}} = 18000$.

6.3.2 Open/closed floodgate

Here the idea is to lower the floodgate when $Q_{\text{before}} \geq 17500$ and to close it again when $Q_{\text{before}} < 17500$. The floodgate is lowered to a fixed level such that $Q_{\text{outlet}} = 500$ when $Q_{\text{before}} = 18000$. This last property yields a relation between d and l. After choosing l (and thus d) we can now plot the function (54) again, for values $17500 \leq Q_{\text{before}} \leq 18000$. Below $Q_{\text{before}} = 17500$ the floodgate is closed and no water leaves the river.

It has to be mentioned that for $l < 7000$, Q_{after} will grow beyond 17500 when $Q_{\text{before}} \geq 18000$, so the corresponding floodgates do not decrease discharge sufficiently in case of an extremely high Q_{before}. In fact $l \approx 7000$ corresponds to the only weir with

$$Q_{\text{after}} = 17500 \text{ when } Q_{\text{before}} = 18000,$$

and

$$Q_{\text{after}} \leq 17500 \text{ for all } Q_{\text{before}}.$$

So it is the only weir that meets the requirement in (49) and also behaves properly for $Q_{\text{before}} \geq 18000$.

6.4 Constructions with flow underneath

Each of the previous configurations had water flowing over the construction, which is necessary for options without control. We now shortly look into the option of flow underneath a closable floodgate or through a pipe, as sketched in Figure 26.

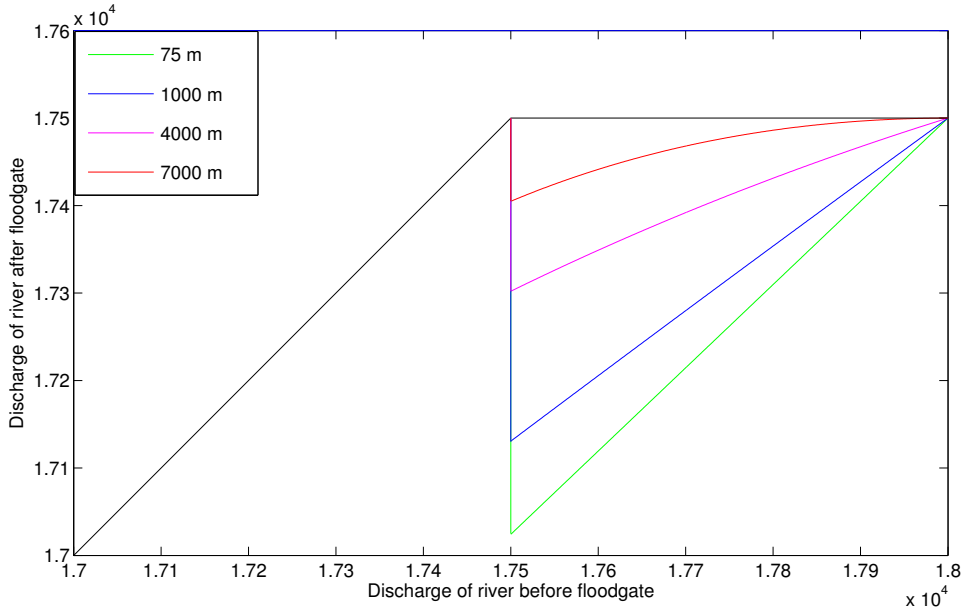

Figure 25: Effect of opening floodgate on discharge in river. For intermediate discharge too much water enters the retention area. This effect is larger for shorter floodgates, which need to be lowered more (see Figure 24). Below Q_{before} all functions coincide with the black line.

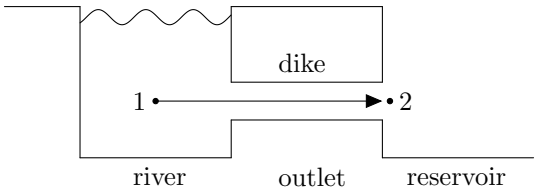

Figure 26: A cross section of the construction with a pipe in the dike. When the pipe is opened water from the river flows through the outlet, e.g. from 1 to 2.

All calculations will be based on Bernoulli's law, which is essentially an energy conservation law along streamlines:

$$\frac{\rho v_1^2}{2g} + \rho z_1 + \frac{p_1}{g} = \frac{\rho v_2^2}{2g} + \rho z_2 + \frac{p_2}{g}, \tag{56}$$

with v the speed of the water flow perpendicular to the river flow, g the gravity acceleration, z the elevation, p the pressure and ρ the density of water. The subscripts correspond with different locations, see Figure 26. The velocity v_1 (perpendicular to the flow of the river) can be assumed to be almost zero. Since the water is horizontally flowing through the pipe, $z_1 = z_2$. Furthermore, p_2 equals the air pressure and the pressure at position 1 may be written as $p_1 = p_2 + \rho g h$, with h the distance between the opening of the pipe and the water surface. Therefore, equation (56) reduces to

$$v_2 = \sqrt{2gh}, \tag{57}$$

which was already derived experimentally by Torricelli in the 17^{th} century.

If the outlet is located at the bottom, the height of the river is given by equation (52). For $Q = 18000$, this means $h = 7.22$. Using equation (57), the velocity is determined,

$$v_2 \approx 12\text{m/s} \approx 43\text{km/h}.$$

For comparison, we estimate the velocity of water flowing through the outlet in both the case of a weir using condition (55) ($h = 0.18$) and a small floodgate as discussed in section 6.3.1 with a length of 75 metre ($h = 3.7$). Using equation (50), we obtain:

$$v_{\text{weir}} = 0.89\text{m/s} \qquad v_{\text{floodgate}} = 4.0\text{m/s}.$$

The speed of the water flowing underneath a floodgate or through a pipe is much larger compared to the situation where the water is flowing over a weir or a floodgate. This may cause more damage for constructions inside the reservoir, but the size of the outlet can be made as small as $\frac{500}{12} \approx 40\text{m}^2$.

6.5 Discussion

Because of the nonlinearity of Q_{after} as a function of Q_{before}, it is not possible to construct a weir with preferred characteristic (49). One is naturally led to weaker requirements ((53) and (55)), of which the latter is preferred because it at least has sufficient inflow into the reservoir. In fact, for a weir, requiring that water starts flowing into the reservoir only at a certain discharge Q_{before}, is not the correct way to view the problem.

In theory, the continuously controlled floodgate fulfills the preferred characteristics of equation (49). Though this construction may be hard to implement in practice, Figure 24 gives an indication of how much a floodgate should be lowered at all possible discharges.

For long weirs or floodgates ($l = 13000$, $l = 7000$), the water levels at $Q_{\text{before}} = 18000$ are only about 12 and 18 centimeter above the weir or floodgate respectively, hence implementation would need a high level of precision. The authors doubt whether any model would be able to predict the required height of the weir with sufficient accuracy. This will certainly be the case for the model we used, as it implicitly assumes the width of the river to be large compared to the length of the outlet.

Compared to the weir, the open/closed floodgate prevents superfluous inflow for $Q_{\text{before}} \leq 17500$. This allows for smaller constructions, although the disadvantages of redundant inflow for $17500 < Q_{\text{before}} < 18000$ and insufficient inflow for $Q_{\text{before}} > 18000$ are more significant.

Even smaller constructions are possible with an outlet at the bottom of the river. However, one needs to take into account the speed of the water exiting the outlet.

7 Conclusions

Discharge levels into the river Rhine at the Dutch-German border are expected to rise due to climate change. Assets and livelihood in the Netherlands are thus at risk unless appropriate measures are taken. The study group working on this problem looked into three aspects of flooding the Rijnstrangen area as a protective measure. First we performed a statistical analysis of the recorded water levels. We found that an extreme discharge is expected to occur every 1250 years and to last for about three and a half days. The Rijnstrangen area was found to be large enough to serve as a buffer for the excess of water. Next, we developed a partial differential equation model for the water flow in the river. Numerical results indicate that the time scale of transient phenomena is small compared to that on which discharge rises and falls. Transients can thus be neglected in the model. Finally the design of passive weirs and active floodgates was investigated. We advise the implementation of the latter option if indeed the Rijnstrangen area is to be used as a retention area.

References

[1] United States Army Corps of Engineers, "Engineering and Design - Flood-Runoff Analysis", Publication number EM 1110-2-1417, Chapter 9, 31 Aug. 1994.

[2] R. Vitolo, P. M. Rutti, A. Dell'Acqua, M. Felici, V. Lucarini and A. Speranza, "Accessing extremes of mid-latitudinal wave activity: methodology and application", Volume 61, Issue 1, pages 35–49, Tellus, 2009.

[3] Stoker: *Water waves: The Mathematical Theory with Applications*, Wiley, 1957.

[4] Hendriks: *Introduction to physical hydrology*, Oxford University Press, 2010.